Potential field cellular automata model for pedestrian flow

Peng Zhang,[1,3,*] Xiao-Xia Jian,[1,3] S. C. Wong,[2] and Keechoo Choi[4]

[1]*Shanghai Institute of Applied Mathematics and Mechanics, Shanghai University, Shanghai 200072, P.R. China*

[2]*Department of Civil Engineering, The University of Hong Kong, Pokfulam Road, Hong Kong SAR, P.R. China*

[3]*Shanghai Key Laboratory of Mechanics in Energy Engineering, Shanghai 200072, P.R. China*

[4]*Department of Transportation Engineering, TOD-Based Sustainable Urban Transportation Center, Ajou University, Korea*

(Received 6 September 2011; published 13 February 2012)

This paper proposes a cellular automata model of pedestrian flow that defines a cost potential field, which takes into account the costs of travel time and discomfort, for a pedestrian to move to an empty neighboring cell. The formulation is based on a reconstruction of the density distribution and the underlying physics, including the rule for resolving conflicts, which is comparable to that in the floor field cellular automaton model. However, we assume that each pedestrian is familiar with the surroundings, thereby minimizing his or her instantaneous cost. This, in turn, helps reduce the randomness in selecting a target cell, which improves the existing cellular automata modelings, together with the computational efficiency. In the presence of two pedestrian groups, which are distinguished by their destinations, the cost distribution for each group is magnified due to the strong interaction between the two groups. As a typical phenomenon, the formation of lanes in the counter flow is reproduced.

DOI: 10.1103/PhysRevE.85.021119 PACS number(s): 05.50.+q, 05.65.+b, 45.70.Vn, 02.60.−x

I. INTRODUCTION

Pedestrian dynamics has been studied for decades, with a large variety of powerful models proposed, including the continuum (or macroscopic) model [1–7], the social force model [8–10], and the cellular automata (CA) model [11–19]. The continuum model adopts hydrodynamic or gas-kinetic equations to describe the behavior of pedestrian crowds. The social force model treats pedestrians as particles and establishes an acceleration for each particle subject to the interactions between these particles. The CA model divides the walking domain into cells and the movement of a pedestrian in an occupied cell to an empty neighboring cell is also divided into time steps for evolution.

The *floor field* model [13–16,18,19], which is a type of CA model, is able to describe many of the remarkable collective behaviors of pedestrian dynamics. The floor field helps all pedestrians to move in a certain geometry to the destination. In general, there are two types of floor fields: the static floor field S and the dynamic floor field D. The static field depends only on the distance measure (from a cell to the destination), and thus S remains unchanged in the evolution. The dynamic field reflects the virtual tracks left by moving pedestrians. On the one hand, the cell (x, y) that a pedestrian leaves becomes empty and attractive, with $D_{xy} \to D_{xy} + 1$. On the other hand, D_{xy} decays and diffuses with certain probabilities (δ and α) so that the cell will not become too attractive to induce too many conflicts or too high densities in the surroundings.

The present paper establishes a cost *potential field* for pedestrian dynamics in the CA model. The cost potential in a cell is defined as the minimal cost for traveling from this cell to the destination. We assume that each pedestrian is fully aware of the surroundings and the destination. Therefore, a pedestrian is able to choose one or more empty neighbors as his or her target cell, which is expected to minimize the traveling cost. More precisely, a target cell is selected such that the pedestrian anticipates a maximal decrease in the cost potential per unit distance in the motion. As a consequence, the pedestrian is always able to arrive at the destination, where the potential is set to be 0.

Two terms referring to the costs of traveling time and discomfort are implied in the cost distribution. Without the discomfort term, the resulting cost potential in a cell would simply measure the distance between the cell and the destination, which is independent of time and similar to the static field in the floor field CA model (or similar to that in [20]). With the discomfort term, the cost distribution increases with the local density, which is reconstructed at each time step and, thus, is time dependent. In this case, the resulting cost potential field is similar to the dynamic field in the floor field CA model. More relevantly, the quickest path or minimal cost for improving the floor field in the CA model was discussed [21,22]. A similar strategy was also used to optimize a pedestrian's path choice in the social force model [23].

However, the cost distribution or potential discussed in this paper is more directly related to the continuum model of pedestrian flow [4–7], which is deterministic in nature. See also [24] and [25] for discussions of similar relations. As a result of this relation or as can be seen from the aforementioned rules, the proposed potential field CA model considerably reduces conflict, as well as randomness, compared with the floor field CA model, although the rules for resolving conflicts are similar. As a consequence, the proposed model is computationally efficient in general.

To describe two pedestrian groups with different destinations, the cost distribution corresponding to each group is multiplied by a magnification coefficient, which takes into account the interaction between the two groups. The magnification in a cell increases according to the "intersecting angle" of the negatives of two potential gradients in the cell. This formulation is largely based on a recent field study [26] and is applied to the reproduction of lane formation phenomena in counter flow, in particular.

We should note that the proposed model, together with those that assume the optimal path-choice strategy, is the

*pzhang@mail.shu.edu.cn

approximation of rigorous rationality, which is able to reproduce reasonable pedestrian flow phenomena in normal situation. However, in principle, human rationality is bounded because of their lack of complete information and ability to compute complex system, their psychological deficiency that inevitably yields errors, and the confliction between decisions, which should be responsible for irregular pedestrian movement and which will be considered in future studies.

The remainder of this paper is organized as follows. In Sec. II, the basic principle together with the floor field used in the CA model for pedestrian dynamics is briefly discussed, as is the cost potential in a continuous domain. In Sec. III, the potential field in a discrete domain is discussed, which is for a pedestrian's path choice in the CA model and helps determine the probability of the pedestrian's moving to an empty neighboring cell. In addition, the potential fields with respect to two pedestrian groups are developed through extension. In Sec. IV, the evacuation of pedestrians is simulated in comparison with the floor field model to indicate the efficiency of the potential field model. The phenomenon of lane formation in counter flow is also reproduced. Section V concludes the paper.

II. THE FLOOR FIELD VERSUS THE COST POTENTIAL

By dividing the walking domain into cells, the CA model assumes that each cell is either empty or occupied by one pedestrian. Suppose that a cell (0,0) is occupied at time step $t = n - 1$, and then the update from step $n - 1$ to step n is implemented with nine probabilities: the pedestrian may keep still or move to one of eight neighboring cells [Fig. 1(a)]. These nine probabilities p_{ij} constitute the matrix M_{ij}, $-1 \leqslant i, j \leqslant 1$ [Fig. 1(b)]. The subsequent issues relate to the determination of p_{ij} and the resolution of conflicts. We assume in advance that a neighboring cell is considered by the pedestrian only if it is empty, that is, we assume that $p_{ij} = 0$, for $(i, j) \neq (0,0)$, if (i, j) is not empty.

A. The floor field CA model

In the floor field CA model, the probabilities shown in Fig. 1(b) are determined by the formula

$$p_{ij} = \tilde{N} \exp(k_D D_{ij}) \exp(k_S S_{ij})(1 - n_{ij})\xi_{ij},$$
$$\tilde{N} = \left[\sum_{i,j} \exp(k_D D_{ij}) \exp(k_S S_{ij})(1 - n_{ij})\xi_{ij} \right]^{-1},$$

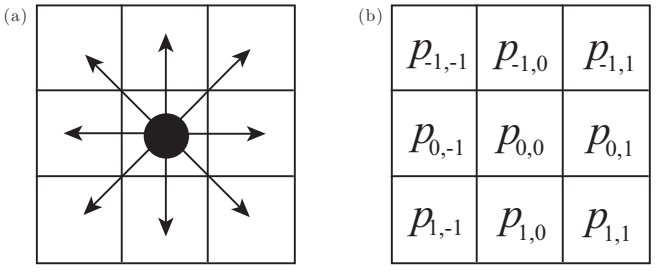

FIG. 1. (a) An occupied cell and its eight neighboring cells, corresponding to (b) the nine probabilities for the pedestrian in the occupied cell to update his or her position.

where the first and second exponentials are related to the dynamic (D) and static (S) fields, respectively, with k_D and k_S being the two sensitivity parameters. It is assumed that $n_{ij} = 1$ for an occupied cell and that $n_{ij} = 0$ for an empty cell, except that $n_{0,0} = 0$ always holds. The number $\xi_{ij} = 1$, except that $\xi_{ij} = 0$, for the cells representing walls or obstacles. Note that $n_{ij} = 1$ or $\xi_{ij} = 0$ implies $p_{ij} = 0$, in which case moving to cell (i, j) is forbidden.

In the static field, S_{xy} is initially defined using some distance metric for all cells, which does not change over the entire evolution. In the dynamic field, the value of D_{xy}, which is initially set to 0 in all cells, can be altered during the update from step $n - 1$ to step n, according to the following rules. If a cell (x, y) has been left by a pedestrian, then the value is updated by $D_{xy} \to D_{xy} + 1$. If D_{xy} has been altered at an earlier step with $D_{xy} \geqslant 1$, then the value decays with probability δ and diffuses with probability α to one of the neighboring cells. As mentioned earlier, the decay and diffusion prevent the cell that a pedestrian has left from becoming too attractive. Moreover, the diffusion allocates more attraction or higher probabilities to the neighboring cells, especially those that have not yet been occupied. The relative probabilities are adopted to resolve the conflict arising from two or more pedestrians having the same target cell.

We refer readers to [13], [14], and [16] for more detailed discussion.

B. The potential in a continuous domain

For the discussion in this section, let (x, y) denote the coordinates in the walking domain. Then the potential $\phi(x, y)$ is associated with the cost distribution $\tau(x, y) \geqslant 0$, such that

$$\begin{aligned} \phi(x, y) &= \int_{(x,y)}^{(x_0,y_0)} \tau(x, y) ds \\ &= \int_{(x,y)}^{(x_0,y_0)} (\tau(x, y)x'(s)dx + \tau(x, y)y'(s)dy), \end{aligned} \quad (1)$$

where (x_0, y_0) is (or belongs to the set of) the destination(s). The integral path is represented by $l : x = x(s),\ y = y(s)$, with $ds = \sqrt{dx^2 + dy^2}$, and the unit vector $(x'(s), y'(s))$ points to the integral direction. To ensure a one-valued function $\phi(x, y)$, we necessarily assume that the integral is independent of the path, i.e.,

$$\phi_x(x, y) = -\tau(x, y)x'(s),\ \phi_y(x, y) = -\tau(x, y)y'(s), \quad (2)$$

which gives rise to the *Eikonal* equation:

$$\sqrt{\phi_x^2(x, y) + \phi_y^2(x, y)} = \tau(x, y). \quad (3)$$

The integration of (1) implies $\phi(x_0, y_0) = 0$, which serves as a boundary condition of Eq. (3). Thus, the Eikonal equation can be uniquely solved by assuming $\phi(x, y) \geqslant 0$. See the discussion in [27] for the numerical solution. These steps guarantee the existence and uniqueness of the potential $\phi(x, y)$.

Given $\phi(x, y)$, Eq. (2) suggests that the integral path be uniquely determined by

$$l : \frac{dy}{dx} = \frac{\phi_y}{\phi_x}, \quad \phi(x_0, y(x_0)) = 0, \quad (4)$$

which shows that the potential $\phi(x,y)$ truly represents a cost that is integrated from (x,y) to (x_0,y_0) along the path l. We indicate that $\phi(x,y)$ is the minimal cost from (x,y) to (x_0,y_0). In fact, the cost along any path reads

$$\begin{aligned}\int_{(x,y)}^{(x_0,y_0)} \tau(x,y)ds &= \int_{(x,y)}^{(x_0,y_0)} \sqrt{(-\phi_x)^2+(-\phi_y)^2}\sqrt{dx^2+dy^2} \\ &\geqslant -\int_{(x,y)}^{(x_0,y_0)} \phi_x dx - \int_{(x,y)}^{(x_0,y_0)} \phi_y dy \\ &= \phi(x,y)-\phi(x_0,y_0)=\phi(x,y),\end{aligned}$$

and the equality holds if and only if $(dx,dy)||(-\phi_x,-\phi_y)$. Assume that a pedestrian at (x,y) moves along the path l so that he or she anticipates minimizing the travel cost from (x,y) to (x_0,y_0). Then, the direction of motion at (x,y) is taken as

$$-\nabla\phi(x,y)=(-\phi_x(x,y),-\phi_y(x,y)), \tag{5}$$

and Eq. (4) defines the streamlines of the flow field.

In the continuum model, the cost distribution depends on the density, which varies with the evolution [4–7], and the formula

$$\tau(x,y,t)=\frac{1}{v_e(\rho(x,y,t))}+g(\rho(x,y,t)) \tag{6}$$

is commonly used [5–7]. The first term in (6) is related to the traveling time, with $v_e(\rho)$ being the velocity-density relationship and $v_e'(\rho)<0$. The second term represents the discomfort of pedestrians, with $g(0)=0$ and $g'(\rho)>0$.

III. THE POTENTIAL FIELD CA MODEL

In the context of Fig. 1, we need to determine the probabilities shown in Fig. 1(b). The determination is based on the potential field, which is essentially an extension or discrete version of the cost potential in a continuous domain (discussed in Sec. II B) and requires reconstruction of the density distribution. These steps are specified in the following discussion.

A. The discrete potential field

Let (x,y) now represent a discrete cell. Then the cost distribution $\tau(x,y)$ is essentially taken as Eq. (6), except that the velocity $v_e(\rho)$ should be replaced by $v_{\max}=1$, according to the basic rules of the CA model. Taking the length and area of a cell as the unit, the maximal density is set as $\rho_{\max}=1$, which is consistent with the assumption that one cell can be occupied by, at most, one pedestrian.

Using these dimensionless variables, and for a fixed time t, we define the cost distribution in a cell (x,y) as

$$\tau(x,y,t)=\frac{1}{v_{\max}}+g(\rho(x,y,t)),\quad 0\leqslant\rho\leqslant 1, \tag{7}$$

where $g(0)=0$ and $g'(\rho)>0$. Obviously, the potential $\phi(x,y,t)$ arising from the first term in (7) is independent of time t and, thus, is completely static. According to the numerical solutions in the discrete cells, the negative gradients of (5) or the streamlines of (4) will roughly point to the destination [27]. In this case, each pedestrian will move directly toward the destination, such that he or she anticipates minimizing the traveling time or distance. Such a potential plays a similar role to the static field in the floor field model. The second term in (7) gives rise to a dynamic potential field, in which the cost of discomfort increases with increased density along the route. Therefore, a pedestrian may detour to avoid empty cells that represent higher local densities, even though they are closer to the destination. The potential arising from this term is similar to the dynamic field in the floor field model. For simplicity of expression, we incorporate the two terms in (7) into one, thereby assuming that

$$\begin{aligned}&\tau(x,y,t)=C(\rho(x,y,t)),\\ &C(0)=1,\quad C'(\rho)>0,\quad 0\leqslant\rho\leqslant 1.\end{aligned} \tag{8}$$

Given the distribution of pedestrians in the surrounding cells, there could be many formulas for the reconstruction of $\rho(x,y,t)$. We consider, at most, the 25 cells that are surrounded by the square centered on (x,y) and simply take the average density as the density in cell (x,y). We note that the outside cells, including those denoting walls or obstacles, together with their areas, are excluded and that the reconstruction is unnecessarily required to obey the mass conservation.

B. Determination of probabilities and resolution of conflicts

By setting $\phi=0$ in the destination cell(s), which serves as the boundary conditions, $\phi(x,y,t)$ in the Eikonal equation (3) can be numerically solved using the fast sweeping method [27]. Here, the discrete values of $\tau(x,y,t)$ are determined by Eq. (8). However, given the potentials $\phi(x,y,t)$ in all cells, it is not appropriate to apply Eq. (5) directly, because the vector might point to an occupied neighboring cell.

Nevertheless, the underlying principle can be reinterpreted so that we can reformulate Eq. (5), which suggests that a pedestrian at cell (x,y) will tend to move to a neighboring cell along the path that minimizes the directional derivative of $\phi(x,y,t)$. The directional derivative of $\phi(x,y,t)$ at (x,y) with respect to a neighboring cell $(x+\Delta x,y+\Delta y)$ can be represented by

$$\begin{aligned}&\frac{\phi_x(x,y,t)\Delta x+\phi_y(x,y,t)\Delta y}{d(\Delta x,\Delta y)}\\ &=\frac{\phi(x+\Delta x,y+\Delta y,t)-\phi(x,y,t)}{d(\Delta x,\Delta y)}+O(d(\Delta x,\Delta y)),\end{aligned} \tag{9}$$

where $d(\Delta x,\Delta y)=\sqrt{\Delta x^2+\Delta y^2}$ is the distance between the centers of the cells (x,y) and $(x+\Delta x,y+\Delta y)$. Therefore, by removing the higher order term $O(d)$, the directional derivatives with respect to all empty neighboring cells can be effectively evaluated by the first term on the right-hand side of (9), thus establishing the minimum of the derivatives. This term is more precisely interpreted as the decrease in potential per unit distance.

To update the positions of all pedestrians from time step $n-1$ to time step n, we set $t=n-1$ in all of the equations involved and, thus, derive all cell values of potential $\phi(x,y)$ at that moment. Then, in the context of (9), the path-choice strategy can be roughly described as follows. A pedestrian will tend to move to an empty neighboring cell to maximally reduce the potential per unit distance; otherwise he or she will

stay put. Moreover, a target cell for more than one pedestrian will be occupied by the one who attains the maximal decrease in potential per unit distance.

Assign (0,0) to each occupied cell. Then the procedure for determining the probabilities p_{ij} shown in Fig. 1(b) is specified as follows.

(1) Compute the difference quotient $\delta\phi_{ij}(0) \equiv (\phi(i,j) - \phi(0,0))/d_{ij}$ for $(i,j) \in S_0 = \{(i,j)|(i,j)$ is empty$\}$, where d_{ij} is the distance between cell (i,j) and cell (0,0).

(2) Define the set $S_m = \{(i,j)|\delta\phi_{ij}(0) = \delta\phi_{\min}(0)\} \subseteq S_0$, where $\delta\phi_{\min}(0) = \min_{(i,j)\in S_0} \delta\phi_{ij}(0)$, and then define

$$p_{ij} = \begin{cases} 1/|S_m|, & (i,j) \in S_m, \\ 0, & (i,j) \notin S_m, \end{cases} \quad \text{if} \quad S_m \neq \emptyset \quad \text{and} \quad \delta\phi_{\min}(0) < 0;$$

otherwise,

$$p_{ij} = \begin{cases} 1, & (i,j) = (0,0), \\ 0, & (i,j) \neq (0,0), \end{cases}$$

where $|S_m|$ is the number of elements in S_m.

An empty cell (i,j) could be a target cell of m $(0 \leqslant m \leqslant 8)$ pedestrians in the m neighboring cells $(0^{(k)},0^{(k)})$, which gives rise to an occupation conflict if $m \geqslant 2$. To resolve a possible conflict, the probabilities for occupation are defined as follows.

$$p(0^{(k)}) = \begin{cases} 1/|S_{mm}| & \text{if} \quad m \geqslant 1 \quad \text{and} \quad (0^{(k)},0^{(k)}) \in S_{mm}, \\ 0 & \text{otherwise}, \end{cases}$$

where $S_{mm} = \{(0^{(k)},0^{(k)})|\delta\phi_{\min}(0^{(k)}) = \delta\phi_{\min}, 1 \leqslant k \leqslant m\}$, and $\delta\phi_{\min} = \min_{1\leqslant k\leqslant m} \delta\phi_{\min}(0^{(k)})$.

We note that this formulation greatly enhances the certainty of the model, which is reasonable because we assume that all pedestrians are well aware of the destination and the surroundings. In other cases, e.g., in the dark or in the case of panic, these rules should be reset to accommodate the situation.

C. Potential fields for two pedestrian groups

Pedestrians with two different destinations in the same walking facility are divided into two groups. In this case, the density distribution is reconstructed and a potential field is established for each pedestrian group. As a consequence, each cell possesses two potential values, denoted $\phi^a(x,y,t)$ and $\phi^b(x,y,t)$, referring to destinations a and b. The determination of probabilities and the resolution of conflicts in occupying empty cells follow the same procedures as those in the foregoing discussion, except that we replace the difference quotient $\delta\phi_{ij}(0)$ by $\delta\phi^c_{ij}(0)$, where $c = a$ or b refers to the pedestrian group being considered. However, we should reformulate the cost distribution, or formula (8), to reflect the stronger interaction arising between two pedestrian groups.

First, we consider the angle $\psi(x,y,t) = -\langle\nabla\phi^a, \nabla\phi^b\rangle$, resulting from the two streamlines l^a and l^b intersecting at (x,y) [see Eqs. (4) and (5)]. Here, the potential gradient $\nabla\phi^c = (\phi^c_x,\phi^c_y)$ and the partial derivatives ϕ^c_x and ϕ^c_y are discretized by the central difference.

Second, we magnify the cost distribution of (8) by the coefficient $L \geqslant 1$, which suggests a stronger interaction or a larger cost with a larger intersecting angle. In other words, $L \geqslant 1$ is increasing with ψ. Moreover, L should also be increasing with the density of the other pedestrian group. Accordingly, we formulate the cost distribution of each pedestrian group as follows:

$$\tau^c(x,y,t) = C(\rho(x,y,t))L^c(\psi,\rho^d), \quad c = a \text{ or } b, \quad (10)$$

where $\rho = \rho^a + \rho^b$, ρ^a and ρ^b are the reconstructed densities of groups a and b, and d refers to the counterpart of group c, i.e., $d = b$ or a, if $c = a$ or b. Formula (10) should be consistent with Eq. (8), such that $L^c(0,\rho^d) = L^c(\psi,0) = 1$. The equalities suggest that the pedestrians in the two groups belong to, or can be viewed as, the same group as either ψ or ρ^d vanishes, which is described by Eq. (8). We assume that

$$L^c(\psi,\rho^d) = \exp(\beta(1 - \cos\psi(x,y,t))(\rho^d(x,y,t))^2), \quad (11)$$

where $\beta = 0.019$ based on a recent field study of the velocity-density relationship of pedestrian streams with an intersecting angle [26].

Finally, the angle value $\psi(x,y,n-1)$, which is used in Eqs. (10) and (11) for the update from time step $t = n-1$ to time step $t = n$, is approximated by $\psi(x,y,n-2)$. The initial value $\psi(x,y,-1)$ is derived by setting $C(\rho(x,y,-1)) \equiv 1$, which implies that the potential fields are static for both pedestrian groups.

IV. SIMULATION

The potential field model is applied to simulate the evacuation of pedestrians and the formation of lanes in the counter flow. In the simulation, the size of a cell can be viewed as 0.4×0.4 m^2, by which the maximal density $\rho_{\max} = 1$ corresponds to 6.25 pedestrians/m^2. Moreover, the velocity $v_{\max} = 1$ and the interval between each time step can be viewed as 1 m/s and 0.4 s, respectively [13,16]. The cost distribution $C(\rho)$ of (8) is given by

$$C(\rho) = 1 + g_0\rho^\gamma,$$

where we set $g_0 = 0.075$ and $\gamma = 2$.

A. Evacuation of pedestrians

We consider a room divided into 18×14 cells, with an additional two layers of fictitious cells outside and an exit at the center of the left side wall. N pedestrians $(N < 18 \times 14)$ are randomly assigned to the inner cells at $t = 0$ for initialization, which suggests a mean density of $\bar{\rho} = N/(18 \times 14)$. In the simulation, the potential field CA model is compared with the floor field CA model. In the latter model, we set $k_S = 10.0$ and $k_D = 1.0$ in Eq. (1) and formulate the static field as follows:

$$S_{ij} = \max_{(i_l,j_l)}\{\min_{(i_s,j_s)}\{\sqrt{(i_l - i_s)^2 + (j_l - j_s)^2}\}\} - \min_{(i_s,j_s)}\{\sqrt{(i - i_s)^2 + (j - j_s)^2}\}, \quad (12)$$

where the set $\{(i_s,j_s)\}_{s=1}^k$ comprises the cells denoting the exit; the last term is the distance between cell (i,j) and the exit, and the first term is the maximal distance for all (i_l,j_l) in the room. Formula (12) is an improvement of that in [14] and [15]; it reasonably suggests that all S_{i_s,j_s} are equal to the maximum of S_{ij} and is, thus, particularly fitted for a wide exit. The decay and diffusion probabilities for the dynamic field (see Sec. II A)

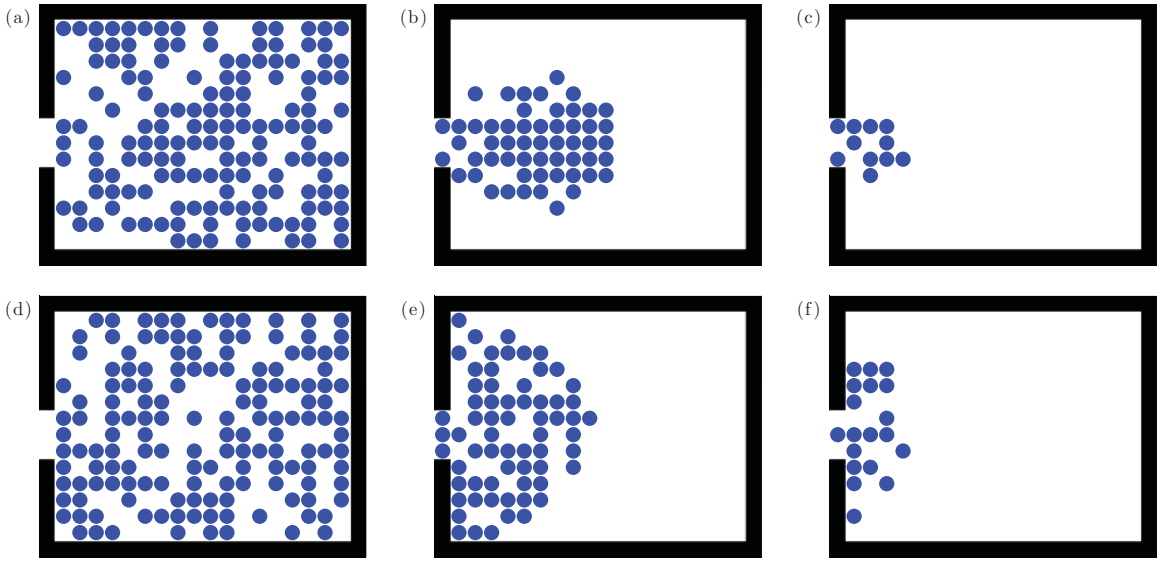

FIG. 2. (Color online) Evacuation process simulated by the potential field model (a–c) and the floor field model (d–f) at $t = 0$, 40, and 60. The average density and the number of cells at the exit are chosen as $\bar{\rho} = 0.6$ and $s = 3$, respectively.

are taken as $\delta = 0.3$ and $\alpha = 0.3$, respectively. See also the discussions in [14] and [15].

Figure 2 shows the evacuation process simulated by the potential field and floor field models. Figures 2(a)–2(c) and 2(d)–2(f) display a similar evolution, except that the evacuation simulated by the potential field model is expected to end earlier than that simulated by the floor field model. This is in accordance with the underlying principle that the path-choice strategy in the potential field model is somewhat optimal due to the pedestrians' awareness of the destination and the surroundings.

The functional relations between the evacuation time and the width of the exit are shown in Figs. 3(a) and 3(b), which are simulated by the potential field and floor field models, respectively. According to these curves, the evacuation time decreases as the width of the exit increases. Moreover, one curve is always above the other, which corresponds to a higher average density, implying that the evacuation time increases with $\bar{\rho}$ for a fixed exit width. These results concur with common sense. In all of these cases, the evacuation time simulated by the potential field model is again indicated to be smaller than that simulated by the floor field model, through comparison of Figs. 3(a) and 3(b). To compare the computational efficiency between the potential field and the floor field models, we alter the walking domain by setting an open entrance on the right side, which is symmetric to the exit on the left side for application of the periodic boundary condition. Figure 3(c) shows that the potential field model takes fewer CPU times generally for a 150-time-step simulation, especially when the average density $\bar{\rho}$ is increasing, which should give rise to many more conflicts in the floor field model.

The potential field model can be conveniently used to simulate the evacuation of pedestrians in a room with any number of exits, simply by setting the potential ϕ to 0 in the cells representing the exits. Figure 4 shows the evacuation process for 600 pedestrians in a room with two exits. These successive scenes display a realistic evolution.

B. Lane formation and jam in pedestrian counter flow

We consider a two-way corridor divided into 60×20 cells, in which the left and right sides are both open to an entrance and an exit. Initially, the corridor is empty and pedestrians begin to enter from the left side with a specific flow (i.e., flow per width) of $\rho_L v_{\max}$. In the meantime, another group of pedestrians begins to enter from the right side with a specific

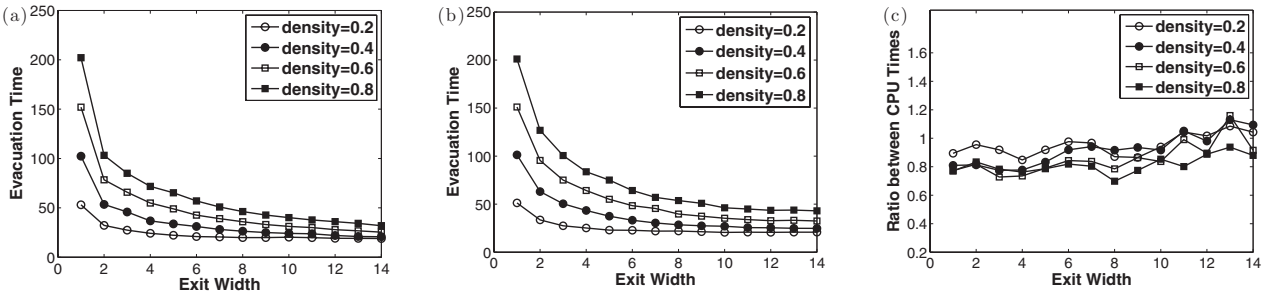

FIG. 3. Functional relations between the evacuation time (steps) and the width of the exit for a variety of average densities $\bar{\rho}$, simulated by (a) the potential field model and (b) the floor field model. (c) Ratio of the CPU times used by the potential field model to that used by the floor field model.

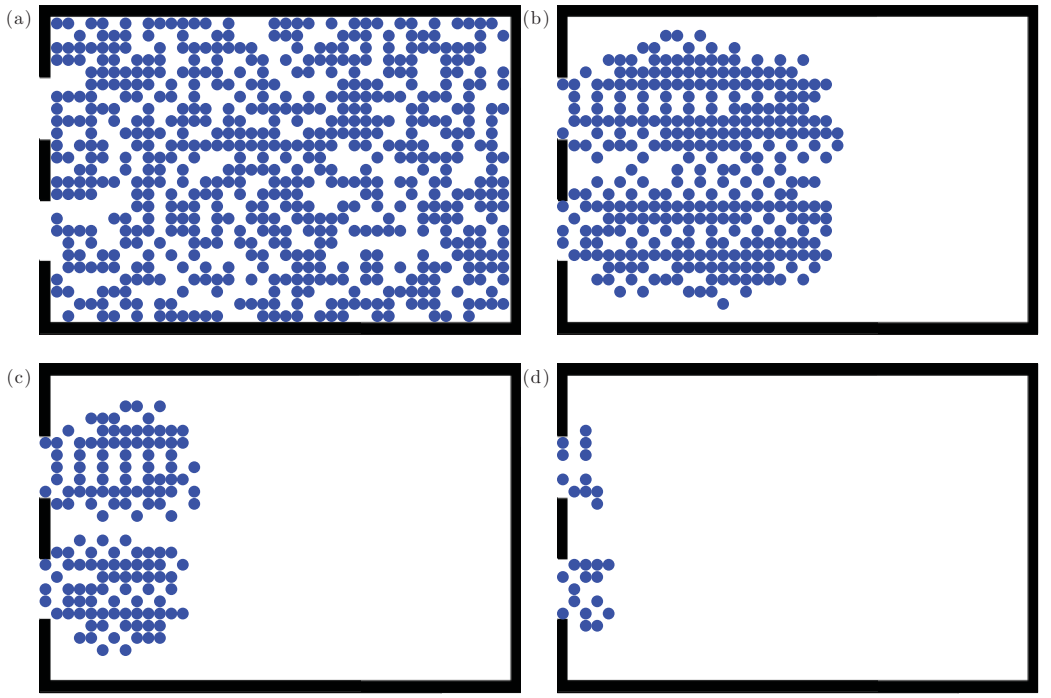

FIG. 4. (Color online) Evacuation of 600 pedestrians ($\bar{\rho} = 0.6$) in a 40×25 room with two exits, each of which includes $five$ cells: (a) at $t = 0$, (b) at $t = 44$, (c) at $t = 72$, and (d) at $t = 91$.

flow (i.e. flow per width) of $\rho_R v_{\max}$. As we set the velocity $v_{\max} = 1$, the density ρ_L or ρ_R is taken as the probability of entrance at each time step, provided that the referred target cell immediately connected to the entrance is not empty. Otherwise, the probability of entrance is set to 0.

By setting $\rho_L = \rho_R$, the potential fields, together with all other operations (including the central difference between ϕ_x^c and ϕ_y^c) on the two pedestrian groups, appear to be completely symmetrical to the vertical line passing along the center of the corridor. Therefore, it appears that a confrontation between the two pedestrian groups at the vertical line is anticipated, and hence a complete block of the corridor. However, we observe the formation of lanes even for high flow rates at the entrances, the evolution of which could last for a sufficiently long time. Figure 5 indicates the simulation results with $\rho_L = \rho_R = 0.18$, by which we retrieve a high entrance flow rate of 0.18 pedestrian/0.4 s = 0.45 pedestrian/s.

The breaking of this symmetrical system is mostly attributable to randomness, especially when one stream of pedestrians encounters the other stream near the vertical line. In the confrontation, an empty cell on or near the vertical line is most likely a target cell of two pedestrians who belong to different groups and possess equal probability of occupation. In this case, throwing a random number determines that one pedestrian occupies the empty cell and the other turns to the left or right (may also be random), which breaks the symmetry. More significantly, Eqs. (10) and (11) suggest that a pedestrian will strongly wish to keep away from the pedestrians in the other group to reduce the traveling cost. As a consequence, a succeeding pedestrian will tend to follow the leading pedestrian in the same group, which gives rise to the formation of lanes after the breaking of the symmetry.

In a study of pedestrian dynamics, the lane formation in a symmetrical system was explained as "noise-induced ordering," which was attributed to the "optimal self-organization" of pedestrians [9,10]. In our case, Eqs. (10) and (11) mostly suggest that the symmetrical system is unstable, and the randomness serves as the "noise" for breaking the symmetry. The optimal principle implied in the potential field then leads to the formation of lanes. An optimal principle based on a cost

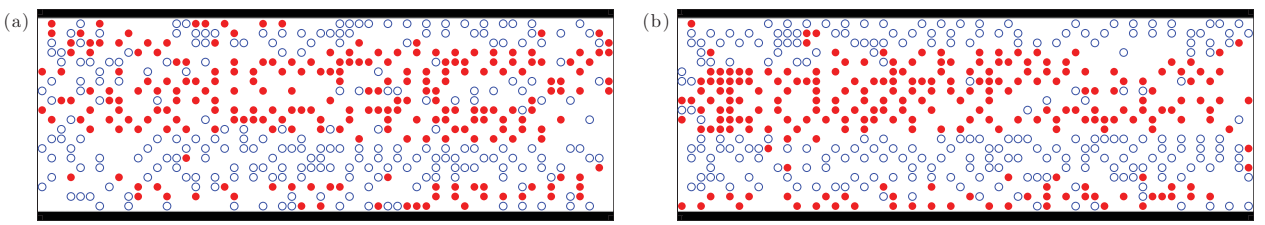

FIG. 5. (Color online) Pedestrian counter flow in a 60×20 corridor with observation of the lane formation phenomenon. Snapshot (a) at the time step $n = 74$ or $t = 29.6$ seconds; snapshot (b) at the time step $n = 100$ or $t = 40$ seconds. Open circles (blue) and filled diamonds (red), respectively, represent rightward- and leftward-moving pedestrians, both of which have an entrance density of $\rho_L = \rho_R = 0.18$.

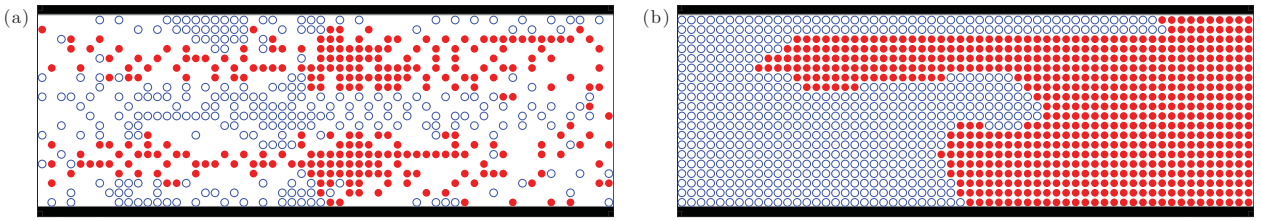

FIG. 6. (Color online) Pedestrian counter flow in the same corridor as in Fig. 5, with the higher density of $\rho_L = \rho_R = 0.2$ at the entrance. Snapshot (a) at the time step $n = 70$ or $t = 28$ seconds; snapshot (b) at the time step $n = 577$ or $t = 230.8$ seconds, when the corridor is blocked completely.

distribution similar to (11) was applied to reproduce the lane formation phenomenon in the continuum model [28], in which case the physics was similar but the numerical viscosity of the scheme was regarded as the "noise" for breaking the symmetry. We note that lane formation phenomena in pedestrian counter flow were also reproduced by the social force model [10], the floor field CA model [13], and the lattice gas model [29].

Finally, Fig. 6 indicates that the corridor eventually becomes blocked with sufficiently high flow rates at the entrances, even though the pedestrians that departed at earlier times are able to arrive at the destinations. The simulation is in accordance with common sense and may help in assigning a limited value for the entrance flow rate for management.

V. CONCLUSION

We develop a potential field for the motion of pedestrians in the CA model. Under the assumption that the pedestrians are well aware of the destination and the surroundings, the potential field suggests an optimal form of path-choice strategy, which considerably reduces the randomness. Accordingly, the proposed potential field CA model suggests a faster evacuation of pedestrians from a room and a shorter computation time than the classical floor field CA model. Moreover, the potential fields for two pedestrian groups traveling in the same walking facility are established, in which we take particular account of the increased interaction between two streams of pedestrians. To avoid this interaction, each pedestrian in the counter flow has a much stronger desire to move away from the other group of pedestrians, which helps with the formation of lanes in the simulation.

As mentioned, human activities essentially deviate from a certain optimization due to "bounded rationality." In a normal situation and for not as dense pedestrian crowds, the deviation might be trivial and thus the optimization could mostly generate an ordering system. However, the deviation could be significant in that it gives rise to irregular pedestrian movement due to extremely high densities or the complex geometry of a walking facility. In this case, the effects of bounded rationality should be taken into account. We refer the reader to [30] for such observed irregular pedestrian movements as the stop-and-go wave and "pedestrian turbulence," together with their evolution into disasters, and to [31]– [33] (and references therein) for study of the car-following model based on the assumption of bounded rationality. We outline the following factors for future studies:

(1) the difference in walking abilities (or speeds) due to differences in age, gender, etc;

(2) the difference in path-choice strategies due to psychological reasons or human attributes;

(3) the specific manner or mood affected by events, which arouses competitive or cooperative movement (e.g., see [34] and references therein);

(4) the complexity in geometry, which should considerably reduce the visibility of all or some pedestrians; and

(5) extremely high densities, which might give rise to or enhance panic among pedestrians.

To model different types of pedestrians, the studies of multiclass vehicular traffic flows in [35]–[37] could be instructive.

ACKNOWLEDGMENTS

The work described in this paper was jointly supported by the National Natural Science Foundation of China (Grant No. 11072141), the National Basic Research Program of China (2012CB725404), the Shanghai Program for Innovative Research Team in Universities, the Research Grants Council of the Hong Kong Special Administrative Region, China (Grant No. HKU7184/10E), and National Research Foundation of Korea rant No. NRF-2011-0000859 funded by the Korea government (MEST).

[1] L. F. Henderson, Nature **229**, 381 (1971).
[2] D. Helbing, Complex Syst. **6**, 391 (1992).
[3] R. L. Hughes, Transport. Res. B Meth. **36**, 507 (2002).
[4] S. P. Hoogendoorn and P. H. L. Bovy, Transport. Res. B Meth. **38**, 169 (2004).
[5] L. Huang, S. C. Wong, M. P. Zhang, C.-W. Shu, and W. H. Lam, Transport. Res. B Meth. **43**, 127 (2009).
[6] Y. H. Xia, S. C. Wong, and C.-W. Shu, Phys. Rev. E **79**, 066113 (2009).
[7] Y. Q. Jiang, P. Zhang, S. C. Wong, and R. X. Liu, Physica A **389**, 4623 (2010).
[8] D. Helbing and P. Molnár, Phys. Rev. E **51**, 4282 (1995).
[9] D. Helbing and T. Vicsek, New. J. Phys. **1**, 13.1 (1999).

[10] D. Helbing, P. Molnár, I. J. Farkas, and K. Bolay, Environ. Plan. B**28**, 361 (2001).
[11] M. Muramatsu, T. Irie, and T. Nagatani, Physica A **267**, 487 (1999).
[12] H. Klüpfel, T. Meyer-König, J. Wahle, and M. Schreckenberg, in *Proceedings of the Fourth International Conference on Cellular Automata for Research and Industry: Theoretical and Practical Issues on Cellular Automata*, edited by S. Bandini and T. Worsch (Springer-Verlag, London, 2000), pp. 63–71.
[13] C. Burstedde, K. Klauck, A. Schadschneider, and J. Zittartz, Physica A **295**, 507 (2001).
[14] A. Kirchner and A. Schadschneider, Physica A **312**, 260 (2002).
[15] A. Kirchner, K. Nishinari, and A. Schadschneider, Phys. Rev. E **67**, 056122 (2003).
[16] A. Schadschneider, in *Pedestrian and Evacuation Dynamics*, edited by M. Schreckenberg and S. Sharma (Springer, Berlin, 2002), pp. 75–86.
[17] Y. F. Yu and W. G. Song, Phys. Rev. E **75**, 046112 (2007).
[18] H. J. Huang and R. Y. Guo, Phys. Rev. E **78**, 021131 (2008).
[19] R. Y. Guo and H. J. Huang, J. Stat. Mech. (2011) P04018.
[20] A. Varas, M. D. Cornejo, D. Mainemer, B. Toledo, J. Rogan, V. Muñoz, and J. A. Valdivia, Physica A **382**, 631 (2007).
[21] T. Kretz, J. Stat. Mech. (2009) P03012.
[22] E. Kirik, T. Yurgel'yan, and D. Krouglov, Cybernet. Syst. **42**, 1 (2011).
[23] T. Kretz, A. Große, S. Hengst, L. Kautzsch, A. Pohlmann, and P. Vortisch, e-print arXiv:1107.2004v1.
[24] T. Kretz, in *Cellular Automata, Lecture Notes in Computer Science*,Vol. 6350, edited by S. Bandini, S. Manzoni, H. Umeo, and G. Vizzari (Springer-Verlag, Berlin, 2010), pp. 480–488.
[25] D. Hartmann, New. J. Phys. **12**, 043032 (2010).
[26] S. C. Wong, W. L. Leung, S. H. Chan, W. H. K. Lam, N. H. C. Yung, C. Y. Liu, and P. Zhang, J. Transp. Eng. ASCE **136**, 234 (2010).
[27] H. K. Zhao, Math. Comput. **74**, 603 (2005).
[28] T. Xiong, P. Zhang, S. C. Wong, C.-W. Shu, and M. P. Zhang, Chin. Phys. Lett. **28**, 108901 (2011).
[29] H. Kuang, X. L. Li, T. Song, and S. Q. Dai, Phys. Rev. E **78**, 066117 (2008).
[30] D. Helbing, A. Johansson, and H. Z. Al-Abideen, Phys. Rev. E **75**, 046109 (2007).
[31] I. Lubashevsky, S. Kalenkov, and R. Mahnke, Phys. Rev. E **65**, 036140 (2002).
[32] I. Lubashevsky, P. Wagner, and R. Mahnke, Phys. Rev. E **68**, 056109 (2003).
[33] I. Lubashevsky, P. Wagner, and R. Mahnke, Eur. Phys. J. B **32**, 243 (2003).
[34] A. Kirchner, H. Klüpfel, K. Nishinari, A. Schadschneider, and M. Schreckenberg, Physica A **324**, 689 (2003).
[35] G. C. K. Wong and S. C. Wong, Transport. Res. A Pol. **36**, 827 (2002).
[36] P. Zhang, R. X. Liu, S. C. Wong, and S. Q. Dai, Eur. J. Appl. Math. **17**, 171 (2006).
[37] P. Zhang, S. C. Wong, and C.-W. Shu, J. Comput. Phys. **212**, 739 (2006).